Panel Location Optimizations for Concentrated Solar Power Tower Systems

Justin Yang

Abstract

Concentrated solar power (CSP) allows for the harnessing of the sun's heat and light for energy. Although it is less common than the other primary method of harnessing solar power, the photovoltaic panel, CSP has advantages over solar panels, such as simpler and cheaper energy storage during the night. In its current form, it is underutilized, and its potential for power generation is immense, with efficiency rivaling that of solar panels. The benefits of CSP come from the fact that solar panels are designed to only absorb photons from visible light, meaning photovoltaics can only harness a very small portion of the vast light spectrum. Panels that can use wavelengths shorter than visible light have vastly increased costs. However, the mirrors used in concentrated solar power can be easily coated with materials that allow for the reflection of a much larger set of wavelengths of light; the energy of all of the photons in this light can be used to generate power in a CSP system. Such mirrors, like ones made of polished aluminum, already have a market and are neither hard nor expensive to procure. Additionally, because the energy transmitted by the CSP mirrors is all heat energy, designers can easily add insulation, providing power losses from heat dissipation of under 1%.

CSP currently has a global installed capacity of only 6.8 Gigawatts[1] versus over 710 Gigawatts for solar panels.[2] This paper seeks to provide an introduction to the basic optical physics that are necessary for understanding CSP, such as light's wave-particle duality and the concept of étendue. Then, this work will model the sun's movement over the course of a year and use it to create equations for constant light reflection onto a specific point. These equations will then be implemented in a simulation to find the best locations for flux transmission.

The main findings of this paper are that from a cartesian plane; panels in the first and third quadrants transmit the most amount of light flux. Additionally, ignoring any light diffusion effects of the mirrors themselves, the further panels are from a central tower, the better their performance. This is hypothesized to be due to the projections of the actual angle of the mirror allowing for a larger surface area from the sun's point of view, therefore transmitting more flux. Future simulation work should include the effects of light diffusion on the panels and expand the grid until placing any more mirrors adds no benefit.

1: Background

1.1: Renewable Energy

In contrast with traditional energy sources such as oil and gas , renewable energy comes from "unlimited" sources. This mainly includes energy sources from earth's natural

cycles such as waves, waterflow, or the wind, but can also include solar energy. Renewable energy has two benefits: it comes from “eternal” sources and processes, and it Firstly, because the energy sources will not run out in any form of human timeframe, it provides long-term solutions, as non-replenishable sources like gas and oil are being expended much faster than we can replace them. These non-replenishable sources also release byproducts, such as carbon dioxide, that are harmful to the environment. Carbon dioxide’s buildup in the atmosphere causes a global greenhouse heating effect, raising sea temperatures and sea levels.[3] Secondly, renewable energy is also clean compared to oil and gas. Oil and gas have to be combusted to produce electricity, while renewable energy can generate usable power by inducing current with electromagnetic fields or light concentration. There is also incentive for an increase in renewable energy generation and storage, as countries such as the United States have pledged to remove carbon emissions from the electricity sector by 2035.[4]

1.2: Solar Energy

Solar energy is a specific type of renewable energy that harnesses light from the sun. Solar energy has several different subcategories that all harvest energy from the sun in different ways. The most common solar power harnessing device is a solar panel . Solar panels generate electricity because light from the Sun displaces electrons in the semiconductors making up the panels, which generates current. Despite their low base cost, these panels are expensive to maintain and require a separate mechanism to store their generated power. However, another solar energy technology, CSP, has benefits. As the name suggests, CSP uses mirrors to concentrate sunlight rather than panels to generate current. Mirrors are also advantageous over solar panels because they reflect almost all wavelengths of light rather than just visible light and infrared, as solar panels.[6]

1.3: Concentrated Solar Power

In CSP, multiple mirrors are used to reflect sunlight onto a common position. The intensity of the light generates high temperatures, similar to a magnifying glass pointing at the ground. These high temperatures are used to warm up a fluid, typically a molten salt with high heat conductivity.[7] After the molten salt reaches the desired temperature, the difference in temperature from the low resting state to the heated state causes the fluid to store energy through its heat. Now, the molten salt’s energy can be used to boil water, which creates steam. This steam spins a turbine, generating power. This is the same system used in other power sources, such as burning coal to generate steam in a coal plant, or heating water to generate steam in a nuclear reactor.

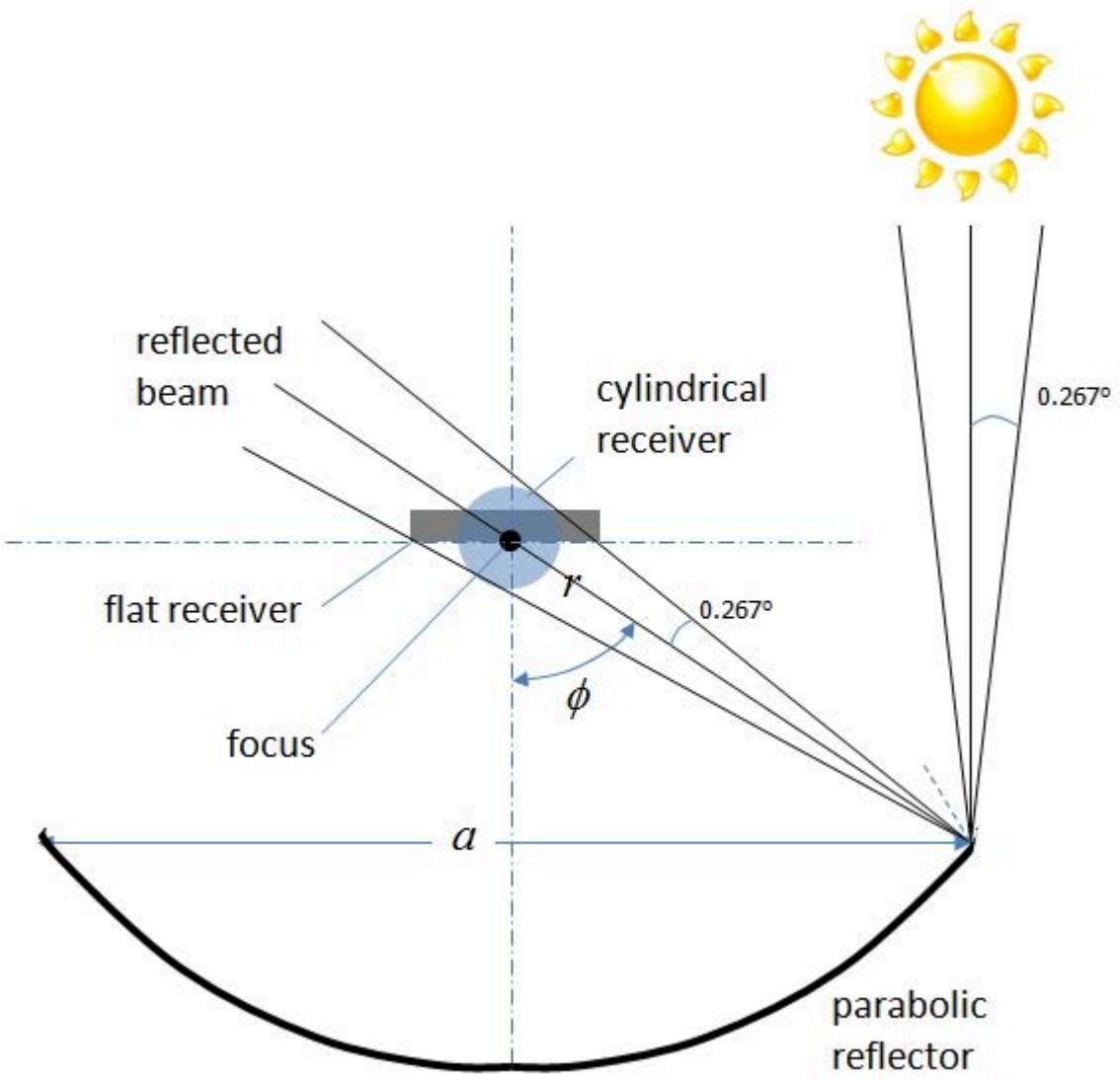

Figure 1: *The above figure shows an example of a cross-sectional view of a parabolic linear trough.*[8]

There are multiple different configurations commonly seen in CSP, such as the parabolic linear trough (Figure 1), in which the mirror is parabolically wrapped around a central tube from which salt flows through. The parabolic geometry of this configuration will be discussed more in section 1.5.

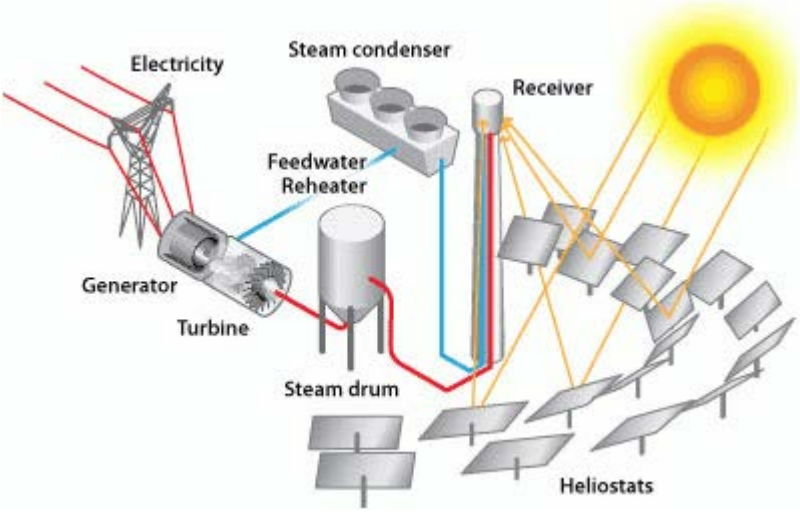

Figure 2: *Above is a diagram of the electricity generation process of a Concentrated Solar Power Tower system. The sunlight is reflected off the mirrors onto the receiver, where the conducting fluid is heated and converted into electricity through a turbine and generator.*[9]

However, in recent years, a new popular design that has emerged is the solar tower, where planar mirrors are arranged around a central receiver tower, and the mirrors reflect sunlight onto the tower (Figure 2). The molten salt is pumped up, heated, and flows down. The solar tower allows for higher light concentration than a parabolic linear trough, which equates to higher temperatures of fluid inside the heating tower. As previously stated, this not only equates to more energy carried by the molten salt, but also through the formula for the efficiency of a heat engine,

$$\%\, eff \;=\; (\,1 \;-\; \frac{low\ temp}{high\ temp}) \;\times\; 100\%$$

this higher temperature allows for a more efficient conversion to electricity, where less power is lost.

1.4: Physics behind optics

1.4.1: Reflection

Another important property of light is how it is reflected off of objects. Reflection occurs because the light, which in this case will be modeled by a particle model of a stream of photons, will physically interact with the molecules that make up an object. Assuming that an object is perfectly flat and reflective, the

incident angle of light will be equal to the angle of the reflected angle, relative across the normal vector to the surface at that point.[5] When looking at a more realistic scenario, small amounts of light scattering do occur but this percentage is rather small, often less than 5%.[10] Additionally, assuming that all incoming light is parallel, because of the properties of reflection, all of the reflected light will also be parallel. Although this allows for the calculation of mirror positions easily, as the reflection angle can be easily calculated, these properties of mirrors raises limitations for the mirror size to achieve an optimal concentration.

1.5: Mirror shapes

1.5.1: Parabolic

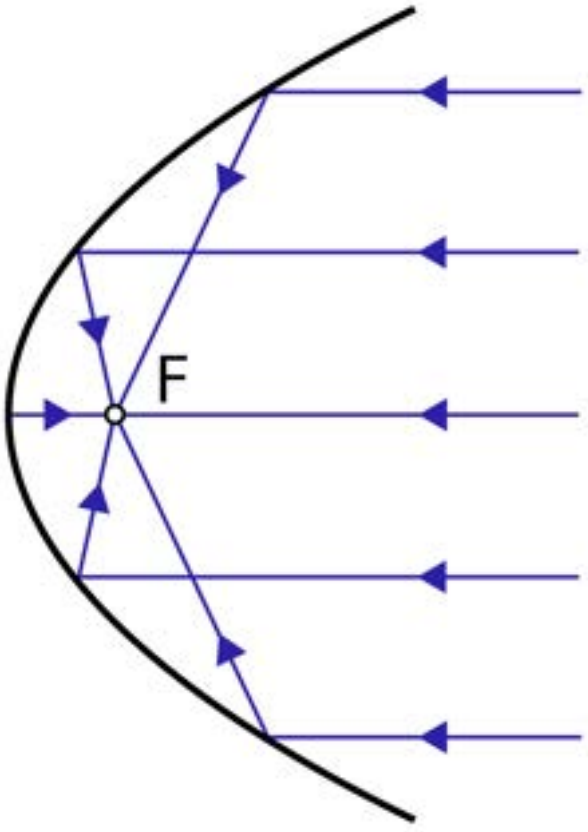

Figure 3: *This Figure displays how sunlight coming in at any angle can be focused by every point on this mirror to reflect to the focal point.*[11]

Parabolic mirror shapes are especially beneficial in their efficacy of concentrating light. This is because of their geometry, where every single reflected ray will contact a single point, the focal point (Figure 3). Therefore, by changing

the shape of the parabola, the distance of the foci to some arbitrary point can be changed as well. Indeed, by increasing the width of the parabola, the reflected vectors will concentrate further away from the parabola.

When making considerations for concentration onto a single receiver tower, such as the scenario with CSP, parabolic mirrors are theoretically the optimal solution, but practically fall short. This is because depending on which ring of mirrors it is in, the distance to the central receiver tower changes, meaning that a single solar tower plant would need a plethora of different mirrors. The manufacturing costs will thus be much higher, on top of the fact that making precisely curved mirrors is already expensive.

1.5.2: Planar

Although planar mirrors are inherently worse than parabolic mirrors at reflecting light due to the fact that all of the reflected light is parallel, because of ease of manufacturing and standardized sizes across mirrors at all distances, they are superior from a cost-effective standpoint. Therefore, in this paper, all of the mirrors involved will be planar.

1.6: Étendue

Étendue is the ability of an optical system to accept light, and it dictates the absolute maximum amount of light that can be gathered. An analogy would be entropy for photons, and its formula is given by

$$G = A * \Omega$$

where G is Étendue, A is the area of the light and Ω is the solid angle of the light source, which in our case is the sun.[12] Étendue importantly cannot be decreased, only increased, which has the practical implications of limiting maximum light concentration. This statement is expressible through the Conservation of Étendue, which states that any system that concentrates more light from some source onto a smaller area must always increase the solid angle of incidence, or the concentrator size.

In CSP, the Conservation of Étendue raises several limitations. It essentially states that more heating will result from smaller mirrors projecting onto a similarly small area of the same size than any other setup. Therefore, in this scenario, reasonably small mirrors of size 1 meter will be used for calculation.

2: Methods

2.1: Modeling the Sun’s behavior

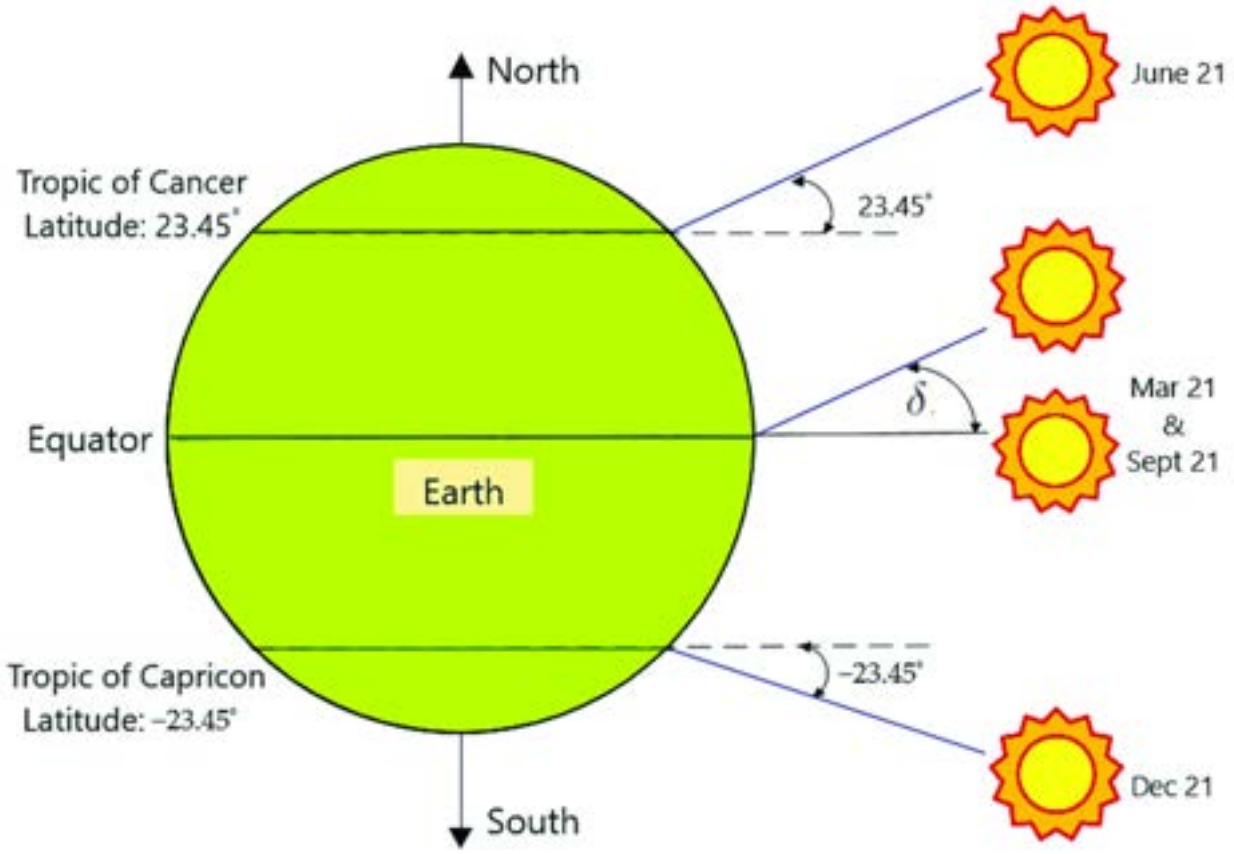

Figure 4: *Above is an image of the solar declination angle, δ, as it changes throughout the year.*[13]

Firstly, a sufficient model for the position of the sun throughout the day had to be created as a model of location and day of the year. A crucial variable that had to be able to be mathematically modeled was the solar declination, or an imaginary angle relating the plane traveling through the earth's equator to the angle to the center of the sun (Figure 4). As this angle directly impacts the duration of a particular area of the earth experiencing sunlight, it changes throughout the year, with a high peak at the summer solstice and a low at the winter solstice. A formula describing the solar declination angle is given as

$$\delta = 23.45\, sin(\frac{360(284+n)}{365})$$

where n represents the day of the year, and where the angle is in degrees.[14] Going forward, unless specifically mentioned, all of the angles will be in degrees. Using the solar declination angle, the angle of sunset and sunrise are calculable through

$$\omega_0 = \frac{180}{\pi} cos^{-1}(-\, tan(\varphi) tan(\delta))$$

where φ is the latitude of the the location and ω_0 is the angle of sunrise and sunset.[13] The location being used will be Death Valley in California, with a latitude of 36.5053891° and a longitude of -117.0794078°.[15] Death Valley is the location used for this model due it receiving some of the highest solar irradiance within the United States[16] and the potential for CSP applications. A negative value for ω_0 indicates that the event occurs before solar noon, where the angle is 0 degrees, thus signifying sunrise, and vice versa for sunset.

To calculate a more precise time after the beginning of the day for sunrise and sunset, an adjuster on the solar noon time is needed. This adjuster, or the equation of time, accounts for a perceived difference between the mean solar time that chronological devices use and the actual time at which the sun is at the highest point in the sky. A simplified formula for the equation of time can be represented by

$$E = 9.87sin(2f) - 7.53cos(f) - 1.5sin(f)$$

where f is the fractional year, a quantity represented by $\frac{360(n-81)}{364}$, with n representing the day of the year.[14] From here, the local noon time in terms of minutes since midnight can be expressed as

$$snoon = 720 - (4(\lambda - E) - 480)$$

with λ representing the longitude of the position.[17] Because the sun moves roughly 15 degrees every hour since it rotates approximately 360 degrees in one day, the sunrise and sunset angles can be represented in hour quantities, relative to solar noon. By multiplying these hour values by the conversion of 60 minutes to 1 hour, and adding them to the time of local noon, the actual times of sunrise and sunset can be calculated.

Seeing that the sun moves 180 degrees from east to west every day, regardless of its actual height in the sky, a simple model for the azimuthal position can be approximated. The calculation of the time difference between sunset and sunrise in seconds allows for the representation of the sun's azimuthal position in the sky as a linear function that travels 180 degrees in this set amount of seconds.

Fractional Year	Equation of time	Solar noon	Sunrise time	Sunset time	Local sunrise seconds	Local sunset seconds
-79.1	-5.9	709.1	421.1	995	25267	59701

For example, on the first day of the year, the difference between the sunset and sunrise time is 34434 seconds, resulting in a slope of 0.00523. This equates to the sun's movement of 0.00523 degrees across the horizon every second. The full table with data for all days of the year can be found here.

2.2: Physics of a reflector

Figure 5: *Pictured above is a side-on view of a panel and how it needs to be angled in order for the reflection of the sunlight to hit the central receiver tower.*

A crude, one-dimensional model of a solar tracker can be made here and serves as an introduction to the geometry of how mirrors reflect light. The end goal of reflecting the sunlight on to a central solar tower provides for a destination in mind for the light. This destination point has an angle given by the height of the central receiver and the horizontal distance from the panel to the tower. Through some simple geometry, the angle in degrees to the tower is:

$$tower\ angle\ = \frac{180}{\pi} tan^{-1}(\frac{\Delta h}{\Delta d})$$

with Δh and Δd being the symbols labeled as such in Figure 5.

The assumed Δh for the model will be 50 meters, a reasonable height for a small-scale CSP plant. While the angle to the tower remains constant throughout a day, the angle of the sun changes constantly between sunrise and sunset. Mirrors also have a property of reflecting light at an identical angle across a plane normal, or perpendicular, to their face.

Therefore, a quantity of importance is the angle of the mirror so that this reflection accurately projects light onto the tower (Figure 5). This variable is defined as:

$$N\ = \frac{(90 - angle\ to\ tower) + angle\ of\ incoming\ sunlight}{2}$$

where N is the angle of reflection across the imaginary normal line.

By adding this to the angle to the tower, the mirror's actual angle is modeled. Due to the mirror being tilted from the perspective of the sun, the actual outgoing flux is not the area of the mirror. There are two projections that must be accounted for, the actual angle of the mirror and the angle of the sun. This is done through a sine scalar of the sun's position, due to its peak at 90 degrees, where $sin(90) = 1$, and a cosine scalar of the actual angle of the mirror from the perspective of the sun, due to it being a dot product projection. For example, the final equation in this case would be:

$$\phi = sin(angle\ of\ incoming\ sunlight) cos(N)$$

where ϕ is the transmitted flux.

2.3: Improved model

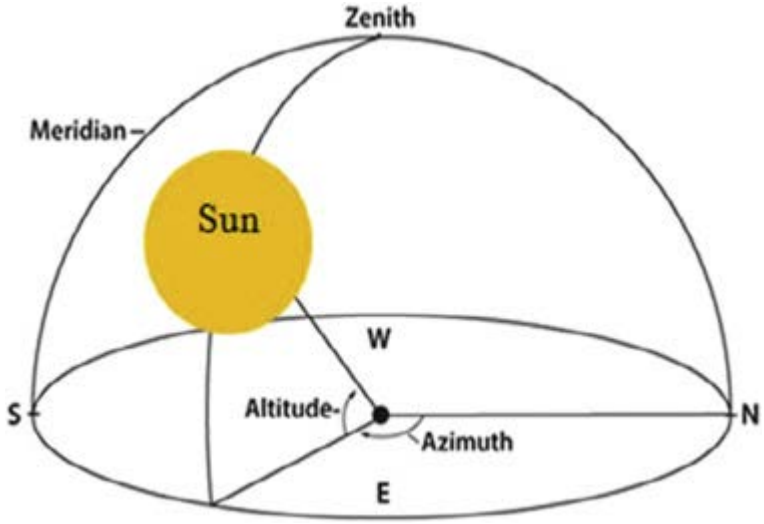

Figure 6: *The above image defines the role of the azimuthal and zenithal angles, where the azimuthal angle represents the movement from east to west, and the zenithal angle represents the height in the sky that the sun reaches.*[18]

The drawbacks of this representation are large. It does not account for the sun's zenithal position, assumes that the panels are all to one side of the central receiver tower, and cannot account for the grid-like nature of real-life CSP tower plants, where mirrors are arranged around the central tower in two dimensions.

Thus, a more accurate, position-independent model must be created, which can easily be done by building on the previous model. Firstly, the zenithal angle, or how high the sun reaches in the sky, must be calculated (Figure 6). This angle is given in radians by the formula:

$$\theta_s = cos^{-1}(sin(\delta)sin(\varphi) + cos(\delta)(cos\varphi)cos(HRA)),$$

where HRA is the hour angle,[17] which converts time into an angle and is given by:

$$HRA = 15(Local\ Solar\ Time - 12)\ ^{19}$$

This allows the creation of a spherical coordinate system, with the sun's position given as two angles on a sphere. Similarly to the previous model, trigonometric scalars must be utilized to account for projections. However, this time there are two sets of projections to be accounted for: the zenith and the azimuthal positions of the sun.

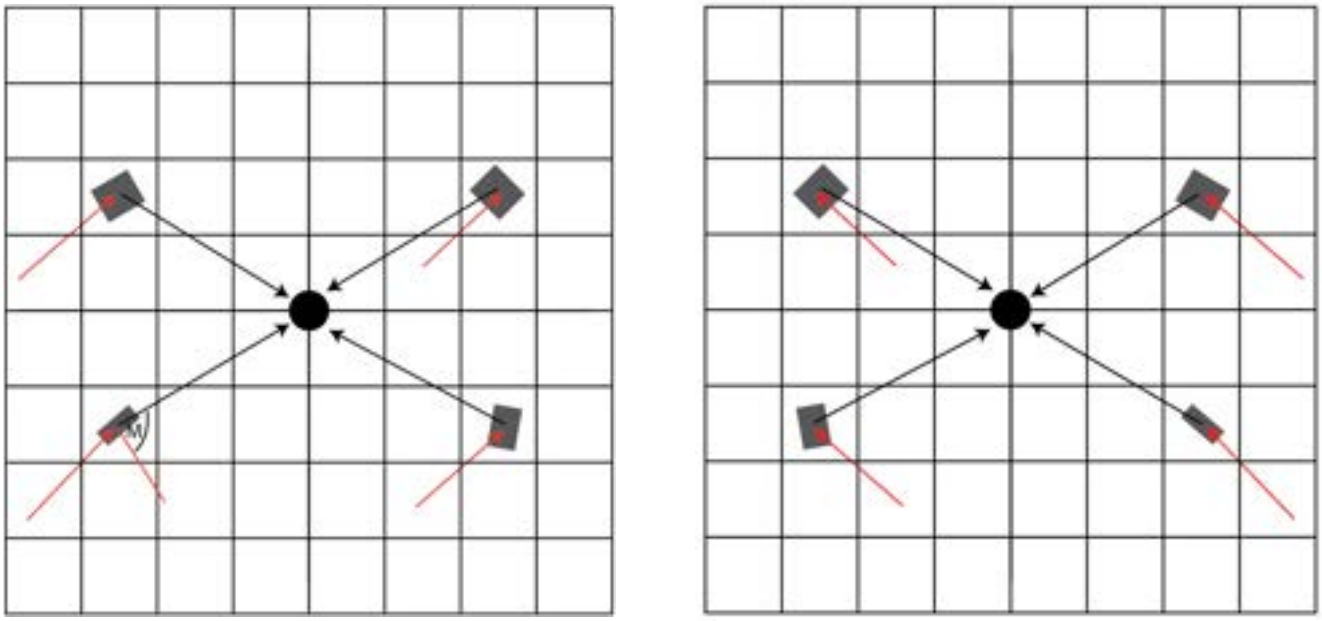

Figure 7: *Pictured are top-down diagrams of the cartesian plane. The diagram on the left represents pre-noon mirror behavior, and the diagram on the right represents post-noon mirror behavior. The red arrows represent the incoming sunlight, the gray squares are the mirrors, and the black arrow is the reflected flux to the black circle, which serves to represent the central tower. Quadrant 1 is the top right, Quadrant 2 is the top left, Quadrant 3 is the bottom left, and Quadrant 4 is the bottom right.*

To represent this, a cartesian plane with four quadrants must be made. Setting the position of the tower as $(0, 0)$ allows us to compute the angle to the central tower relative to an imaginary horizontal line bisecting the grid. Here, the different sectors represent different mirror behaviors that occur in each quadrant (Figure 7), thus changing the half angle as seen as M in Figure 7 and how it is computed. Then, this angle's dot product is taken. Finally, to deal with any potential discrepancies, the function is put through an absolute value function, as the scalar is what matters more than the sign since the transmitted flux can never be negative, only positive or zero. This all results in a final scalar term of $|cos(M)|$: when the angle to the sun is perfectly aligned with the angle to the central tower, the cosine term is maximized, as the half angle does not affect transmitted flux.

The side view scalar calculations given by the zenithal angle remain the same as before (Figure 5), with some minor changes. The main change is that the distance to the tower is now computed with the Pythagorean theorem, given the two dimensional space that everything rests in.

Furthermore, when the sun crosses the point of noon, the formulas necessary for each quadrant must be flipped with the quadrant across from it. Once all of the different

possible situations have been accounted for, the model is complete. For ease of calculation, a Python program was written, where each of the panel locations was modeled as its own grid square. Another benefit of the python program is that it allows us to check for impossible situations. For example, if any of the half angles are larger than 90 degrees at any point, the python program can simply set the transmitted flux to zero, as such a situation would be geometrically impossible.

However, because of limited computational resources and time, a cluster method was implemented. This method takes the previous grid square method and tests how large the grid squares can be with relatively low error. Each of the grid squares would thus enclose a larger area with multiple panels.

Ultimately, the maximum possible movement was determined to be 2 meters in any direction, which will be discussed more in Section 4. Within this 2 meter by 2 meter space, roughly three 1 square meter panels can be fit. This allows for a simplification of computations, as the flux values of all three panels in a grid square can be assumed to be identical.

3: Results

3.1: Flux throughout the year

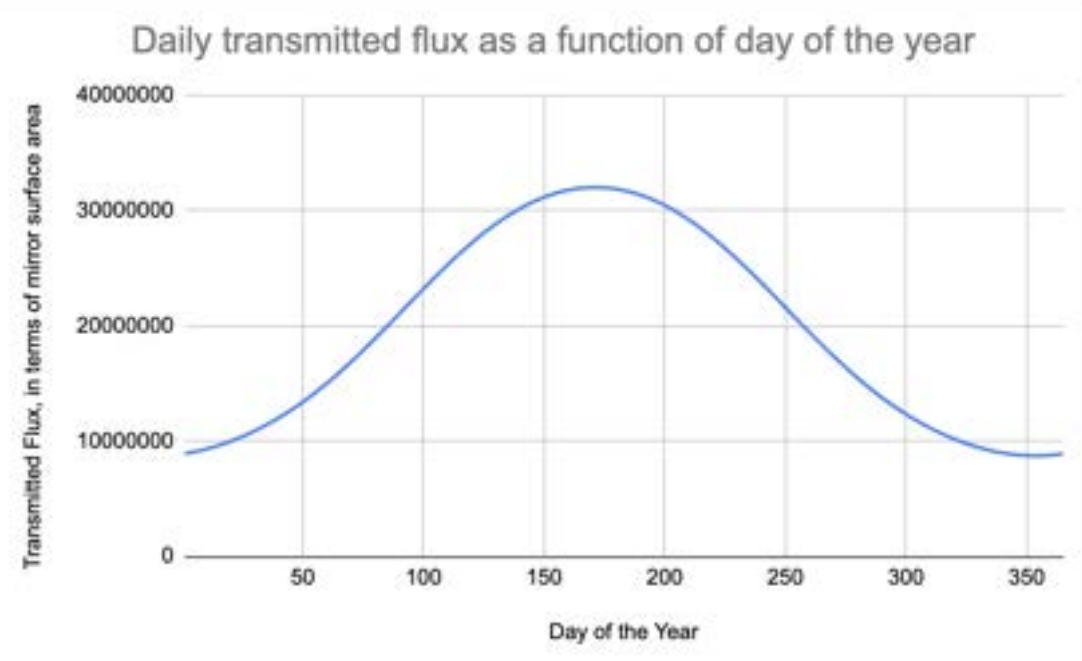

Figure 8: *Pictured above is a graph of the predicted transmitted flux per day as a function of the day of the year in Death Valley, California. Attached is a link to the table with all of the exact transmitted flux values.*

The daily transmitted flux shown in Figure 8 follows a pseudo-sinusoidal form, where it reaches its peak around halfway through the year. This roughly matches the trend of day length throughout the year, reaching a peak during the summer solstice and reaching a low during the winter solstice. Additionally, it also matches with the trend of the solar declination angle and the solar zenithal angle.

3.2: Effect of location on flux generation

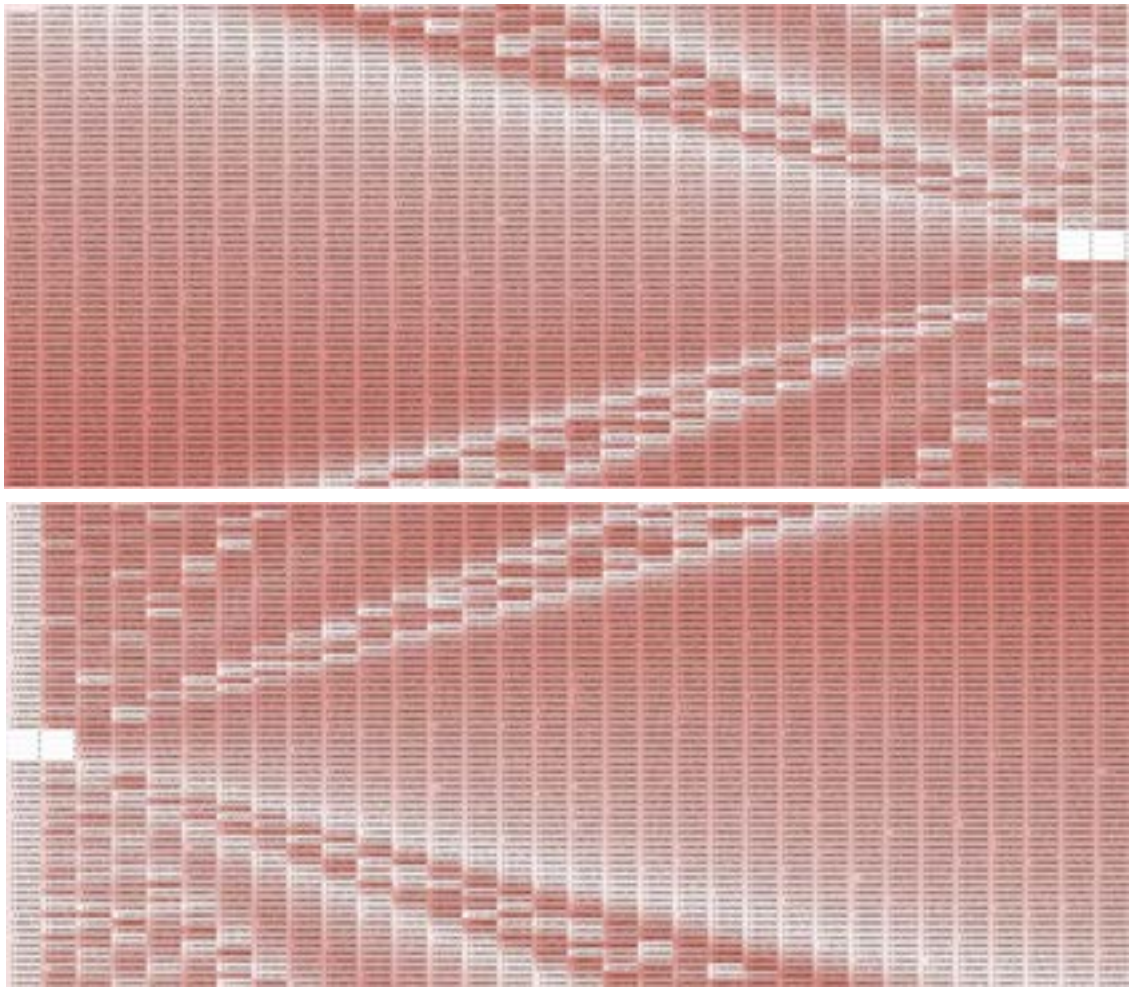

Figure 9: Above is a heatmap for flux generated at specific positions. The redness of a cell dictates its flux generation relative to the rest of the locations in the grid, with a redder

cell having higher transmission, while a whiter cell has comparably less generation. The white grid cells in the center are blank because they denote the theoretical size and location of the central receiver tower.

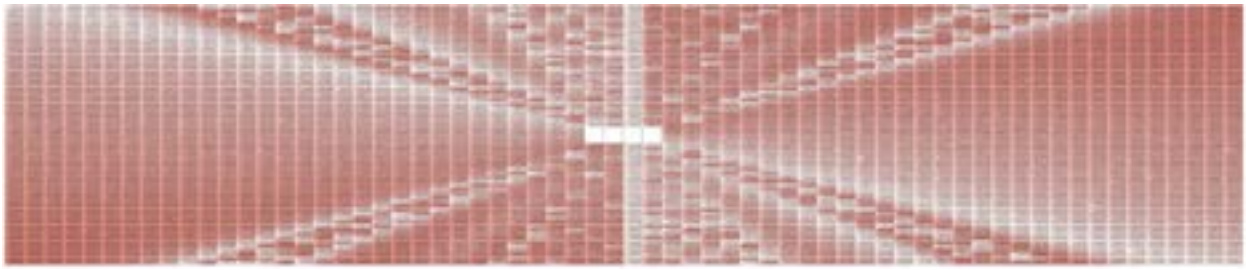

Figure 9 continued: Above is a heatmap that is not broken apart into multiple images. with the attached link to the spreadsheet as well.

The heatmap in Figure 9 shows a clear trend that from the top down, cumulative flux generation peaks in the first and third quadrants. Looking at specific values that are collinear to each other (i.e straight lines of values), high flux values are generally increasing the further out they are from the location of the central receiver tower, while lower flux values are decreasing.

This is because when calculating for the actual transmitted flux, the half angles must be accounted for. Panels further away have a much smaller vertical angle relative to the tower, and therefore, when the sun is higher in the sky and peak solar flux transmission time occurs, the ensuing half angle is smaller than if the panel was closer to the tower. Since the angle when the panel was closer to the tower would already be closer to $90°$, the sun being higher in the sky would mean that the half angle would also be closer to $90°$, leading to a smaller cosine scalar.

In contrast, an unexplained anomaly happens along the 45 degree axes, where there is a noticeable decrease in flux, which is not expected because it is not a continuous decrease, as seen in other areas. Some explanations include incomplete physical modeling, errors in the calculation code, or some physical phenomenon. Future work should analyze this behavior.

The path of the sun has a large effect on the transmitted flux; in some panel locations, the location of the sun causes them to have geometrically impossible locations to transmit flux at certain times. This is reflected in how certain areas, such as the second and fourth quadrants, have theoretically optimal distances, but their actual transmitted flux values are low compared to the rest of the grid.

3.3: Optimal mirror placement

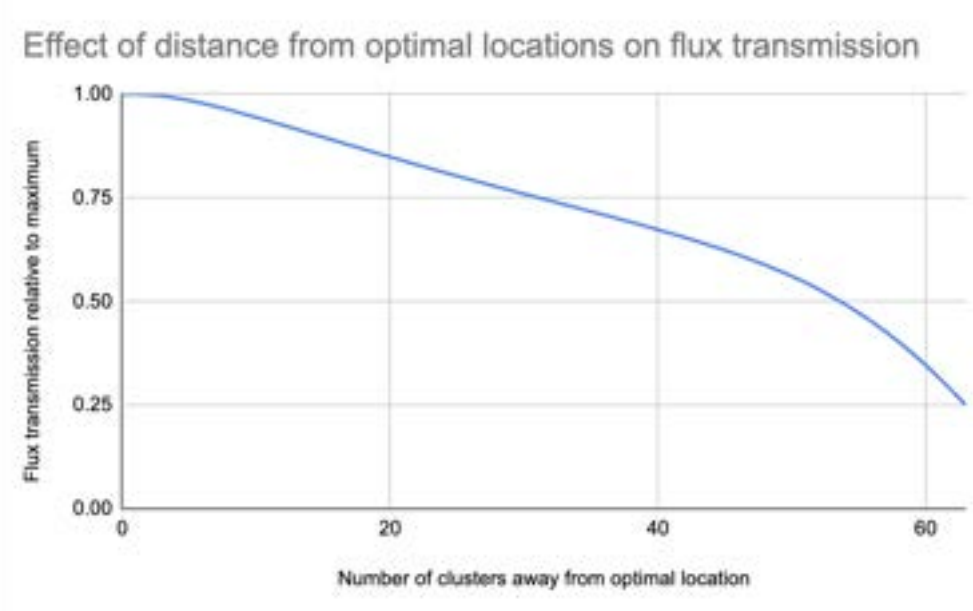

Figure 10: *The above is a graph which compares the number of clusters away a group of mirrors is from the optimal location versus the flux transmission at that location relative to the maximum in the row.* [Data can be found in this table.]

With a limited number of mirrors, the best locations to place them would be thus in the first and third quadrants as denoted by Figure 9, with mirrors further from the central receiver tower seeing more of a benefit, as indicated by the heatmap. In these quadrants, at medium to long distances, the mirrors transmit 60% more flux than the mean of the entire grid. Moving further away from these locations, such as moving up towards the second quadrant corner, appears to linearly decrease the relative flux transmission of a panel until roughly 40 clusters of distance away from the “corner” mirrors, or approximately 80 meters away, as seen in Figure 10. From this point onwards, the transmitted flux sharply decreases to around a quarter of the best-performing location. The performance decreases by 25% at 30 clusters away the “corner” mirrors.

4: Error Analysis

Although error mitigation was attempted as much as possible by adjusting models and comparing to real-life empirical data, due to the complexity of the calculations, assumptions about and simplifications to the model had to be made.

Firstly, a significant possible source of error is the assumption that the mirrors would never interfere with one another. On an imaginary and completely flat plane, mirrors would certainly interfere with each other, whether through their shadows or because of obstructions

when reflecting to the central receiver tower. This would decrease the transmitted flux, but in a real-world system, this can be mitigated by a slight staggering of heights.

The total flux was also computed with a cluster method, in which every single panel in a certain area was assumed to have the same transmitted flux. This approximation is another source of error. For testing the probable upper bounds of the error, a single panel location ten meters from the central receiver tower along the imaginary horizontal axis was selected. This was because closer panels would see larger variation in angle, thus impacting their transmitted flux more. Testing for the maximum size attainable with under 10% of error, movements of 5 meters closer and further in the horizontal direction proved to provide similar results, with 0.42% error when moving 5 meters closer and 0.64% error when moving 5 meters further away. Movements in the vertical direction returned much higher errors; moving "up" 5 meters gave an error of 30%, while a movement of 2 meters gave an error of 9.72%. This vertical movement ultimately decided the size of each of the clusters to be a 2 meter by 2 meter square.

Additionally, another critical assumption for simplicity in this model is that the sun is a point charge, when in reality, it occupies a certain angle of the sky. The sun's solid angle would therefore cause some scatter in the reflected light. On closer reflectors, this poses little issue because the angle does not cover enough distance for any of the light to not hit the central receiver tower. But for further panels, there is the possibility that the solid angle causes some of the transmitted light to scatter and miss the central receiver tower's heating portion, decreasing the transmitted flux. This is especially critical since flux generation appears to maximize at a point further from the central receiver tower. But as scatter depends on distance, this could be accounted for by adding in an additional scalar based on distance during the computational phase.

This model also assumes that the mirrors and weather are perfect, with no zero light diffusion from the mirrors themselves and zero non-sunny days. This assumption is extremely idealistic. However, for our purposes, because any anomaly in the weather conditions would cause a negative effect regardless of configuration and mirror quality, weather conditions do not affect different setups differently, and it can therefore be ignored.

Lastly, all of the mathematical models were completed with the assumption that the earth follows a circular orbit around the sun. Thus, the computed times for sunrise and sunset, which determine the angular speed of the sun throughout the day (as well as the solar declination angle used to compute the zenithal angle of the sun), could all possibly be slightly inaccurate.

5: Conclusion

This paper has provided an introduction to the physics behind CSP tower systems. By calculating the transmitted fluxes at different locations, this model has determined the optimal locations to place solar panels. Generally, the first and third quadrants around the central receiver tower have locations that produce the most flux, with a spike of light transmission in the

summer months when the sun is higher in the sky. Given these trends, a favorable pattern that maximizes the output with a fixed number of panels would be a one-sided, asymmetrical solar tower system, where a majority of the panels are concentrated in a corner of the grid with high energy production. Introducing height staggering of the panels could further enhance the efficiency by preventing overlap. Given the computational resources, computing the cluster method's difference from the actual transmitted flux would serve to enhance and make the error analysis much more thorough. It would also be beneficial to implement a feature in the code that uses the distance from the central receiver tower of the panel to determine what percentage of the light would scatter and miss the tower, thereby accounting for the properties of the mirror. Additionally, with more computational power, the simulation could be made larger, allowing for an effectiveness fallout point to be found, as it is likely that due to the computations with the half angle, the effectiveness of panels could still increase beyond the limits of the 64 by 64 grid.

Citations

1. CSTA (2022), Blue Book of China's Concentrating Solar Power Industry 2021, China Solar Thermal Alliance (CSTA), Beijing, https://www.solarpaces.org/wp-content/uploads/Blue-Book-on-Chinas-CSP-Industry-2021.pdf. Accessed 5 July 2024.
2. IEA. "Solar." *IEA*, International Energy Agency, 2023, www.iea.org/energy-system/renewables/solar-pv. Accessed 5 July 2024.
3. The United Nations. "Causes and Effects of Climate Change." *United Nations*, United Nations, www.un.org/en/climatechange/science/causes-effects-climate-change#:~:text=As%20greenhouse%20gas%20emissions%20blanket,the%20usual%20balance%20of%20nature. Accessed 5 July 2024.
4. Jordan, Greg. "Area Lawmakers Vow to Fight Biden's Clean Power Plan 2.0: U.S. Senator Shelley Moore Capito of West Virginia." *Shelley Moore Capito*, Shelley Moore Capito, 26 Apr. 2024, www.capito.senate.gov/news/in-the-news/area-lawmakers-vow-to-fight-bidens-clean-power-plan-20#:~:text=President%20Joe%20Biden%20has%20pledged,and%20economy%2Dwide%20by%202050. Accessed 5 July 2024.
5. Science Mission Directorate. "Wave Behaviors" NASA Science. 2010. National Aeronautics and Space Administration. http://science.nasa.gov/ems/03_behaviors. Accessed 5 July 2024.
6. "What Wavelength Do Solar Panels Use? The Ultimate Answer." *ShopSolar.Com*, Shop Solar, 22 Oct. 2023, shopsolarkits.com/blogs/learning-center/what-wavelength-do-solar-panels-use#:~:text=Solar%20panels%20are%20designed%20to%20absorb%20light%20in%20the%20visible,400%20nm%20and%201100%20nm. Accessed 5 July 2024.
7. "What Is Concentrated Solar Power and How Does CSP Work?" *Brunel*, Brunel, 10 May 2023, www.brunel.net/en/blog/renewable-energy/concentrated-solar-power. Accessed 5 July 2024.
8. Fedkin, Mark. *Figure 2.7. Geometry of a parabolic reflector. All rays parallel to the parabola axis are reflected through the focal point. 2.4 Concentration with a Parabolic Reflector*, Penn State University, https://www.e-education.psu.edu/eme812/node/557. Accessed 5 July 2024.
9. Solar Energy Technologies Office. *Diagram of the multiple processes and steps in a Concentrated Solar Power tower, including light gathering and conversion to electricity*. *Office of Energy Efficiency & Renewable Energy*, United States Government, https://www.energy.gov/eere/solar/power-tower-system-concentrating-solar-thermal-power-basics. Accessed 5 July 2024.

10. Thorlabs. “Protected Silver Mirrors.” *Protected Silver Mirrors*, Thorlabs, Inc., www.thorlabs.com/newgrouppage9.cfm?objectgroup_id=903. Accessed 5 July 2024.
11. Filu. *Image of light rays reflecting off of a parabolic mirror*. *File:Parabolic Mirror-Diagram.Svg*, Wikimedia Commons, https://commons.wikimedia.org/wiki/File:Parabolic_mirror-diagram.svg. Accessed 5 July 2024.
12. R. J. Koshel, editor, Illumination Engineering: Design with Nonimaging Optics, author of three chapters (IEEEWiley, New York, NY, 2013).
13. Matius, Maryon Eliza & Ismail, Mohd Azlan & Farm, Yan & Amaludin, Adriana & Radzali, Mohd & Fazlizan, Ahmad & Muzammil, Wan Khairul. (2021). On the Optimal Tilt Angle and Orientation of an On-Site Solar Photovoltaic Energy Generation System for Sabah’s Rural Electrification. Sustainability. 13. 5730. 10.3390/su13105730.
14. Bengston, Harlan H. *Solar Energy Fundamentals*, Continuing Education and Development, Inc., www.cedengineering.com/userfiles/Solar%20Energy%20Fundamentals-R2.pdf. Accessed 5 July 2024.
15. “GPS Coordinates of Death Valley National Park in United States. Latitude: 36.5054 Longitude: -117.0794.” *Latitude.to, Maps, Geolocated Articles, Latitude Longitude Coordinate Conversion.*, Latitude.to, latitude.to/map/us/united-states/natural-parks/19/death-valley-national-park. Accessed 5 July 2024.
16. Englert, Michael. “Death Valley: The Mojave Low Lands.” *ArcGIS StoryMaps*, Esri, 8 Mar. 2021, storymaps.arcgis.com/stories/59a85022cfa74e4191ffd7bf317a9341. Accessed 5 July 2024.
17. NOAA. “General Solar Position Calculations.” *General Solar Position Calculations*, National Oceanic and Atmospheric Administration, gml.noaa.gov/grad/solcalc/solareqns.PDF. Accessed 5 July 2024.
18. Kalogirou, Soteris A. “Solar Thermal Systems: Components and Applications—Introduction.” *Elsevier eBooks*, 2022, pp. 1–25. https://doi.org/10.1016/b978-0-12-819727-1.00001-7. Accessed 5 July 2024
19. Zerubavel, E., and R. M. Milne. *Solar Time*, PVEducation, www.pveducation.org/pvcdrom/properties-of-sunlight/solar-time. Accessed 5 July 2024.